

Influence of Pre-Stressed Parts in Dummy Modeling - Simple Considerations -

Ulrich Franz*, Peter Schuster**, Sebastian Stahlschmidt**

*DYNAmore GmbH, Langlingen, Germany

**DYNAmore GmbH, Stuttgart, Germany

Corresponding author:

Ulrich Franz

DYNAmore GmbH, Office North, Im Balken 1

29364 Langlingen, Germany

Tel: +49-(0)5082/9140051, Fax: +49-(0)5082/9140049

E-mail: uli.franz@dynamore.de

Abstract

New regulations and consumer tests for passive safety in passenger cars have increased the demand on accurate models for occupant analysis. Thus, effects that have been neglected or modeled rather coarsely in recent occupant models might necessitate a more detailed modeling in order to capture the dummy behavior sufficiently accurate.

This paper contributes to the discussion of the importance and the modeling techniques of pre-stressed parts in dummy models for occupant analysis. The authors present solutions provided by LS-DYNA to handle the pre-stressed parts like mapping, pre-simulation, or implicit time-stepping for positioning. Finally, the paper discusses sources of pre-stress in different parts of side impact dummies (SID), Hybrid III adult and child dummies. With simple examples the influence of the pre-stress is estimated.

Introduction

One source for pre-stressed parts in dummies is an elastic deformation during positioning, mainly forced by gravity forces. The second main source are parts that are pre-loaded during assembly. An example for such a pre-stressed part is the lower spine of the USSID dummy. It consists of a massive rubber cylinder with a steel cable in its center. During assembly the cable is used to compress the cylinder by 15mm. The pre-stressed cylinder is then assembled between the thorax module and the pelvis. For the recent USSID dummy model [2] the pre-stress in the spine is modeled rather coarsely by using the geometry based on the pre-loaded part. The material properties are adapted such that the model behaves like the pre-stressed part in a component test, although the initial stresses are not considered. Obviously, this is not exact for non-linear problems.

Illustrative examples for deformations of a dummy due to gravity loading are the HIII child dummies. The child dummies have soft lower spines and necks. Hence, the position of a dummy is determined by the position of the limbs and the bending in the neck and the lower spine. Figure 1 depicts two typical initial positions proposed by Lund [11] for out-of-position airbag deployment load cases. In both positions the bending of the neck and spine is significant.



Figure 1: Seating positions according to TWG proposal.

Even for adult dummies gravity leads to remarkable deformations, e.g. the ES-2 dummy shows a difference of 25 mm for the distance between the H-Point and the neck between a model based on CAD data and a measurement of the dummy. Figure 2 depicts a dummy during measurement of key points on the left. On the right hand side the model based on CAD data (yellow) and based on the measurement are plotted against each other. The differences result from bending in the spine and neck, compression loads, and removed clearance.

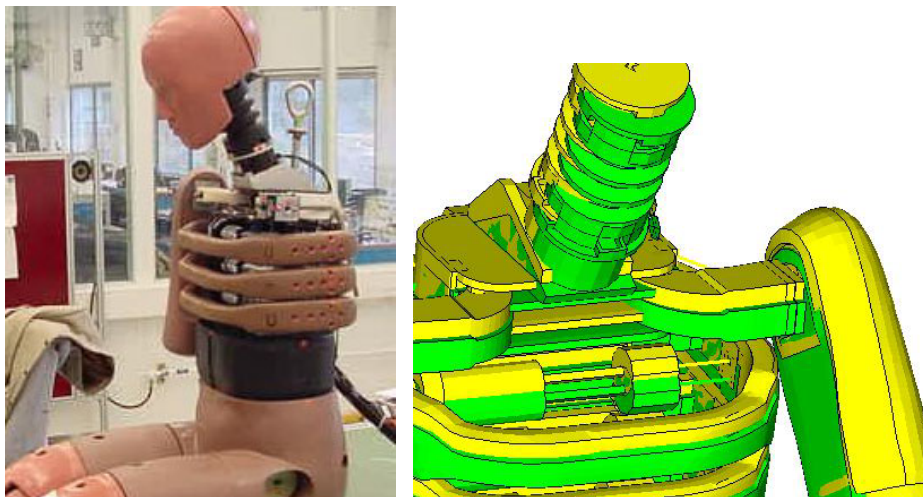


Figure 2: ES-2 dummy (left), dummy model based on CAD data in yellow and model under gravity load in green (right).

Since the seating positions of adult models do not vary significantly the deformation can be determined accurately once and for all. Then a model with a “real” geometry can be used. For in-

stance the recent adult models of the SIDIIIs and the ES-2 model provide an adapted geometry. Usually the initial stresses are neglected in these models.

The demands on the occupant analysis rise steadily. Formerly, occupant criteria used to assess the safety of a vehicle were mainly based on accelerations and intrusions. These quantities are less difficult to predict than forces and moments, see Franz [6]. New regulations like the FMVSS 208 or recent consumer tests take into consideration also force and moment criteria. These types of signals depend strongly on the relative movement of dummy parts against each other. Hence, the modeling of pre-stressed parts that connect parts of the dummy might necessitate a more detailed modeling regarding initial stresses as in the past.

This paper presents features provided by LS-DYNA to determine more accurate initial conditions. Furthermore, the possibilities to include the conditions at the beginning of a dynamic load case are discussed. The described methods are used to analyze the importance of pre-stressed parts in selected examples. The investigations are performed with predictive dummy models from DYNAmore [2, 3] and FTSS [7, 8].

Numerical Possibilities

The proper initial geometry is necessary for an accurate occupant simulation. If deformation is involved in the initial geometry a pre-simulation has to be performed. Based on the pre-simulation different possibilities are available to include the stresses and strains as initial conditions for the dynamic load case. Features provided by LS-DYNA to address these issues are presented next.

Initial geometry

Deformation induced by gravity loading happens slowly. Depending on the load case the event might last longer than one second. Even if the elongations and strains are small the problem is still highly nonlinear due to the multiple contacts in the dummy model. Addressing the problem with an explicit time-stepping is extremely time-consuming. Since many years the implicit time-stepping algorithm of LS-DYNA is used in metal forming applications to predict deformations of the blank due to gravity. Regarding occupant analysis the problem is more complex than in metal forming since much more material models are involved and the contact situation is more complex.

Employing LS-DYNA 971.1477 (double precision) it is possible to determine the initial position of the HIII 3yr model [8] with only a few minor modifications on the dummy model. Figure 3 shows a dummy model before (left) and after (right) the implicit simulation to determine the exact seating position. The duration of the event was 300 ms, the average time step was close to 1 ms; this is factor 1000 larger than in the explicit simulation. The Newmark time stepping scheme with parameters that provide damping was used. The time step was determined automatically and limited to 1.5 ms. No contact modification on the dummy models were needed. Only minor modifications were made to achieve convergence, e.g. element formulations.

All in one run

A simple approach to include the pre-stress is to determine the initial conditions at the beginning of each dynamic load case. This means that the pre-simulation is part of each run. Usually, a huge amount of runs with different parameters and designs are needed to develop a restraint system. The initial conditions are often the same for each run. Hence, the same pre-simulation at the beginning of each run is very time-consuming. More promising would be an approach with a separate pre-simulation followed by final dynamic runs that include the once determined initial conditions. An obvious advantage of the method is that it is very simple and straight forward. The method is used below to consider the pelvis foam of the HIII 50% model [7].

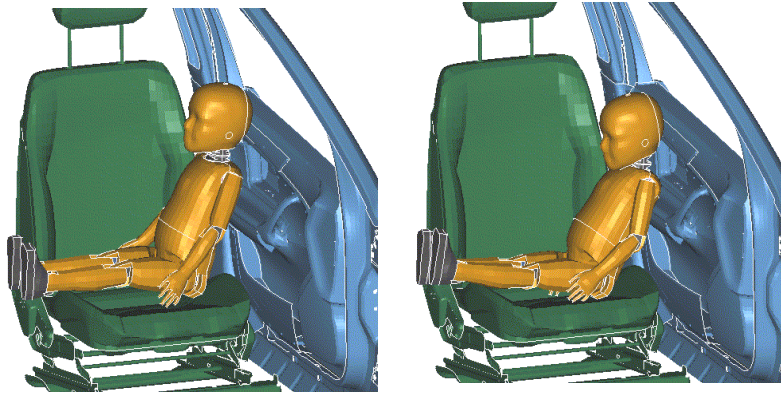


Figure 3: HIII 3 year child model [8]; initial positioning with a preprocessor (left), followed by an implicit simulation (right) with LS-DYNA.

Dynain

In metal forming applications the forming history is included by using the keyword `*INTERFACE_SPRINGBACK`. It generates the file “dynain” containing stresses of selected parts. A mapping of the results on viscoelastic or hyperelastic materials is not yet implemented in LS-DYNA.

Reference geometry

The keyword `*INITIAL_FOAM_REFERENCE_GEOMETRY` allows to include stresses at the beginning of a simulation for many soft foams and rubber constitutive equations. For that feature the deformation gradient is evaluated based on the un-deformed geometry. The method is very easy to handle, stresses of a part can be taken into account by including a file with additional nodal coordinates of the un-deformed geometry of the part and by setting a flag in the material cards. A disadvantage is that the method is limited to hexahedron elements. This method was used below to consider the neck of the ES-2.

Dynamic relaxation

The keyword `*CONTROL_DYNAMIC_RELAXATION` provides an elegant way to combine the initial loading with the 2nd dynamic load case. Hence, it might be used to carry out a pre-simulation effectively. Furthermore, the keyword also provides a feature to perform a stress initialization for small strains. Therefore a prescribed geometry is given in a D3DRLF file. LS-DYNA then applies the displacement to the different nodes incrementally in the first 10 time-steps. The disadvantage of the latter method (D3DRLF) is that the method is not applicable to rigid bodies.

DYNAtools plot2bc and rbdout2bc

Using the command `*BOUNDARY_PRESCRIBED` with a death time it is also allowed to move the model during the first milliseconds to its known initial position. The small programs `plot2bc` and `rbdout2bc` from the DYNAtools [1] define automatically the boundary conditions based on `d3plot` files and the `rbdout` file. The method involves some pre-processing steps but allows a high flexibility in including the information from previous runs. The method is not limited to small strains and can be used for rigid bodies.

Restart

The keyword `*STRESS_INITIALIZATION` allows to include stresses in a model by using the full restart capabilities of LS-DYNA. This method provides a huge freedom to initialize accurately parts with stresses and strains. The simulation of the dynamic load case needs the input deck of the dummy model and the `d3dump` file of the pre-simulation, as well as the input files of the dynamic load case. This method was used below to consider the neck of the HIII 3yr child model.

Assessment of Influence of Pre-stress and Pre-strain

In the following an assessment on importance of pre-stress and pre-strain for dummy modeling is presented on selected examples. The results of the simulations are summarized in tables. Each example closes with a brief discussion.

Pre-stress in the USSID spine

The USSID is equipped with a spine consisting of a rubber tube with a steel cable in the symmetry line. The steel cable is used to compress the spine up to 15 mm before it is assembled in the dummy. The spine is validated as an assembled component in a pendulum test similar to the test depicted in Figure 9. A simple test allows assessing that the influence of the spine on the occupant injury criteria is limited. We consider 4 model variations of the USSID model [2] in two load cases, the plane and the pelvis barrier as depicted in Figure 4.

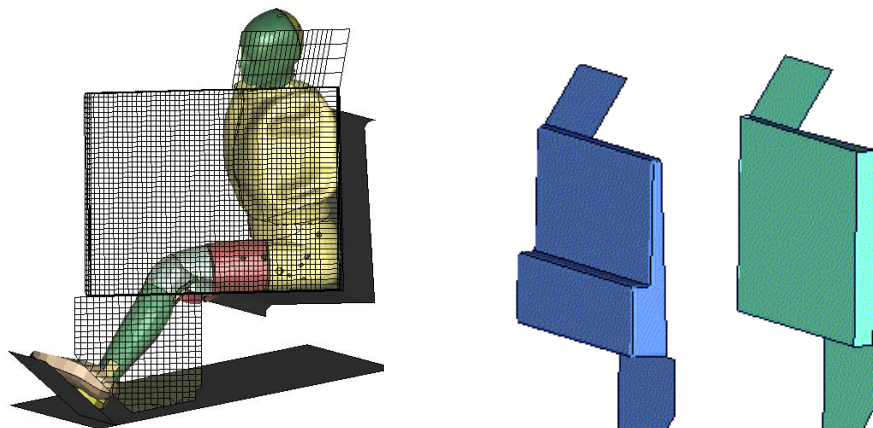


Figure 4: FAT USSID model (left), pelvis barrier model (middle) and plane barrier (right).

Four model variations are considered. Model A is the USSID release [2] with no modifications on the spine. In model B the spine is disconnected to the pelvis cast. In model C the rubber ma-

terial is modeled 2 times stiffer, model D is equipped with a spine 10 times stiffer. The results are outlined for the flat barrier and pelvis barrier in Table 1 and Table 2, respectively.

Accelerations [g], fir Filter	Upper rib	Lower rib	T12	TTI	Pelvis
Model A	46.2	48.7	37.3	43.0	42.6
Model B	46.2	48.5	35.7	42.1	37.5
Model C	46.2	49.3	37.7	43.5	42.9
Model D	46.4	50.9	38.4	44.7	43.2

Table 1: Max. accelerations of FAT USSID model during impact of plane barrier.

Accelerations [g], fir Filter	Upper rib	Lower rib	T12	TTI	Pelvis
Model A	73.2	76.0	61.7	68.9	72.2
Model B	71.0	75.8	57.8	66.8	74.0
Model C	74.3	73.1	63.6	68.5	71.5
Model D	67.3	66.2	70.6	68.4	73.2

Table 2: Max. accelerations of FAT USSID model during impact of pelvis barrier.

For each barrier the signals do not vary significantly for all model variations. The TTI in the pelvis barrier test is changing less than 4%. For the plane barrier the deviation is only 3%. The results show that the material properties of the model of the USSID play a minor role for the occupant injury criteria. Consequently, a more detailed modeling of the pre-stress in the lower spine is not necessary.

Pre-stress in the pelvis foam of HIII 50%

To assess the influence of initial foam deformations of the HIII 50% dummy model a simple test is selected. A cubic block with 50 mm edge length, meshed with tetrahedron elements type 10 with element edge size of 5 mm. The material properties of pelvis foam of the HIII 50% model from [7] are used. The cube is in contact at the bottom with a plate (red). The foam block is then pre-loaded by a plate (blue) from the top and later impacted by a bowl. The test setup is depicted in Figure 5.

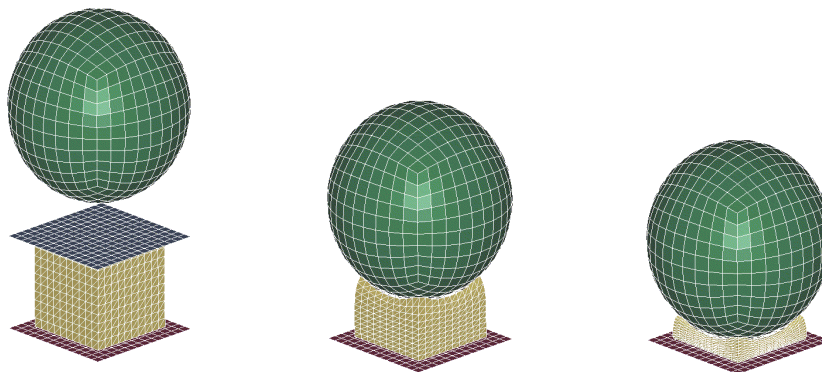


Figure 5: Simple test to estimate influence of initial foam deformation. The foam block not deformed (left), during compression (middle) and maximum compression (right).

The impact speed of the bowl is 8 m/s. The mass of the bowl is adapted such that the maximum bowl deceleration is approximately 50g, 40g, 30g, and 20g for the not pre-loaded foam. The deceleration of the bowl is calculated for different initial strains of the foam block. For each strain the bowl acceleration is determined for two scenarios. One scenario includes the initial stresses, the other neglects the initial stresses. The results are summarized in Tables 3 to 6. If the foam block was not able to absorb the kinetic energy of the bowl entirely, i.e. the calculation terminated due to largely distorted elements, the letters NA were given in the table. Figure 6 shows the maximum compressions of the foam block for the considered load levels.

Bowl deceleration [g]	0 % pre-strain	5% pre-strain	10 % pre-strain	20% pre-strain
initial stress included	44.7	45.4	46.2	50.0
initial stress neglected	44.7	56.7	NA	NA

Table 3: Bowl decelerations for 2.4 kg bowl mass.

Bowl deceleration [g]	0 % pre-strain	5% pre-strain	10 % pre-strain	20% pre-strain
initial stress included	36.2	36.4	36.7	38.6
initial stress neglected	36.2	40.1	48.6	NA

Table 4: Bowl decelerations for 2.1 kg bowl mass.

Bowl deceleration [g]	0 % pre-strain	5% pre-strain	10 % pre-strain	20% pre-strain
initial stress included	27.5	27.6	28.3	30
initial stress neglected	27.5	30.0	32.9	40.3

Table 5: Bowl decelerations for 1.4 kg bowl mass.

Bowl deceleration [g]	0 % pre-strain	5% pre-strain	10 % pre-strain	20% pre-strain
initial stress included	18.7	18.7	19.8	22.2
initial stress neglected	18.7	19.6	20.7	23.6

Table 6: Bowl decelerations for 0.4 kg bowl mass.

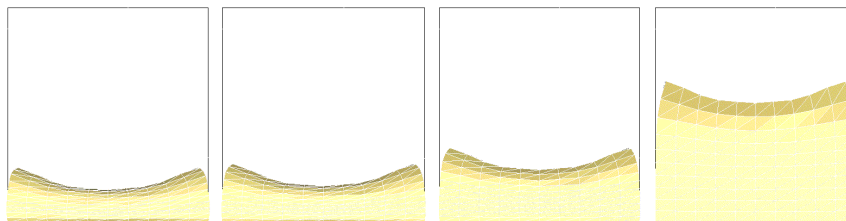


Figure 6: Maximum deformation of foam for bowl masses: 2.4, 2.1, 1.4, 0.4 kg (from left to right). All foams with no initial strain. The black line indicates initial size of the foam specimen.

The simple experiment shows that the influence of initial stress and deformation is more important for high compressions than for low load impacts. The more the load reaches the densification point of the foam the more important the initial condition gets. Even if the results are consistent with a typical stress strain curve for compression of reversible soft foams the authors did not expect that the examples would show such high sensitivity. In particular if initial strains are included and the initial stresses are neglected the bowl acceleration will increase significantly. For example increases the bowl maximum deceleration by 46% for a bowl weight of 1.4 kg and an initial strain of 20% if the initial stresses are neglected. Neglecting both, initial strains and stresses yield a difference of less than 10%, only. Hence, for the example it would be more accurate to neglect the deformation at all, instead of working with a model that includes the strains only. The conclusion is also valid for medium compression load cases of this foam, as outlined in Table 4. For low compression load cases as in Table 6 the effects do not play a significant role and can be neglected.

Pre-stress in the ES-2 neck

The neck of the ES-2 dummy consists of three main parts, the head/neck interface plate, neck/torso interface plate and the central moulded section with two linking plates. The two linking plates and the interface plates are connected by a joint in the center. The movement of the two plates against each other is limited by 4 section buffers at the top and 4 at the bottom linking plates. The buffers are available with different shore hardnesses to tune the neck to comply with its required performance. The neck and the buffers are depicted in Figure 7. During assembly the buffers are pre-stressed, as depicted in Figure 8.

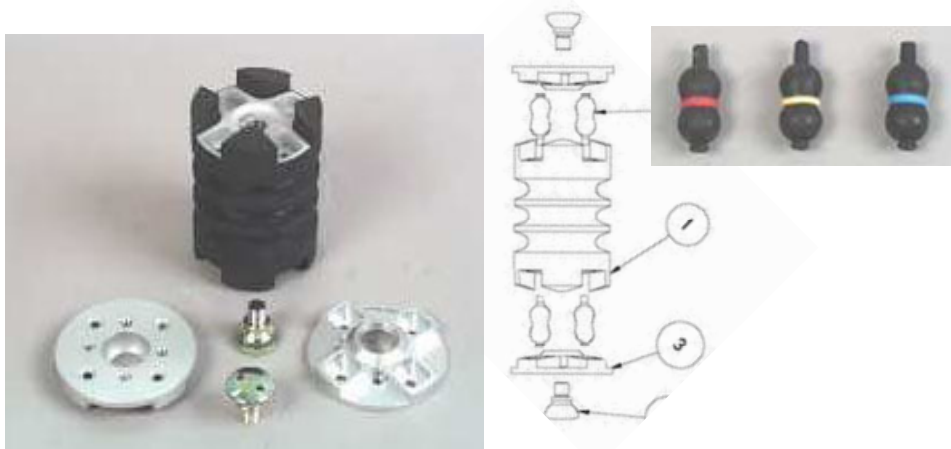


Figure 7: Disassembled parts of neck of ES-2 (left) [12]. Assembly is outlined in drawing (center), buffers (right).

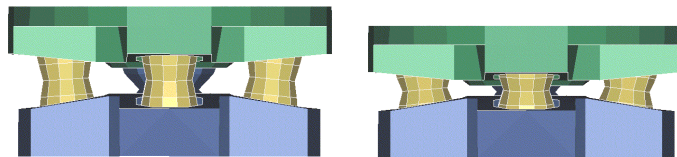


Figure 8: Model of upper interface plate and linking plate with buffers, before final assembly (left) and after assembly (right).

To estimate the importance of stresses in the buffers an extended neck model of the FAT ES-2 model [3] was used. The stresses in the buffers are determined by a pre-simulation. For the dy-

dynamic load case the command *INITIAL_FOAM_REFERENCE_GEOMETRY was used to include the initial stresses. For the study a modification of the calibration pendulum test was chosen. The pendulum is depicted in Figure 9. The reason not to use the calibration test was to consider lower bending angles and a changing of the signs of the forces and moments. The pendulum is positioned vertically and is accelerated in the first 20 ms by a pulse. The pulse has a linear descending slope and crosses the x-axis at 10ms; after 20 ms the pulse is set to 0. Different maximal accelerations were chosen to achieve different load levels. The rotating angle of the pendulum is very small, even for the high load pulse it is below 5 degree. For the different load cases the y-force measured in the neck force transducer range from 125 N to 550 N, and the x-moment range from 6 Nm to 90 Nm. For all considered load cases no influence of the pre-stressed buffers on the neck forces were observed. Even for very low load levels no influence is obvious. Actually, if the model neglects the contact between the parts of the central unit that contact the adapter plate during bending (see mark 1 and 3 in drawing of Figure 7) no major influence of pre-stress was present in this test. The observation is valid for all 3 buffer types. In summary the examples show that the pre-stress in the buffers of the ES-2 neck has no significant influence in the considered load range.

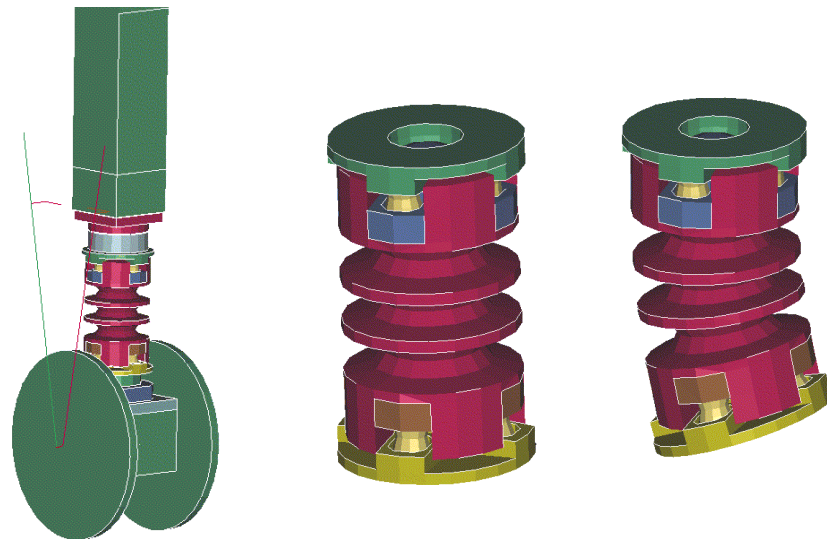


Figure 9: Neck model mounted between pendulum and head form (left). Neck with initial geometry (middle) and neck during test (right).

Pre-stress in the HIII 3 year child neck

To estimate the importance of initial stresses for the neck of the HIII 3 yr child model a sub model of the model [8] is employed. The sub model consists of the head and neck and spine model. The spine is orientated angularly in space. A pendulum is used to impact the chin with a velocity of 6 and 4 m/s. The mass of the pendulum was adapted to obtain relevant load levels for neck moments and forces. Table 7 and 8 summarize the results if the spine is fixed in space. Tables 9 and 10 present results obtained by removing the constrained of the spine and increasing the density of the spine to achieve a spine weight of approximately 13 kg. Four different neck models were analyzed. Model A has a straight neck, as depicted in Figure 10 on the right. The neck of model B is adapted by a “virtual” joint, as depicted in Figure 11 on the left. The curvature of the neck has been determined by a pre-simulation for models C and D. The geometry of the neck is depicted on Figure 11 on the right. Model D does include the initial stresses, model C does not. Table 7, 8, 9 and 10 summarize the neck forces and moments as well as head and pen-

dulum accelerations. Since during simulation the moments change the signs the minimum and maximum values are given. The simulation time was 20 ms.

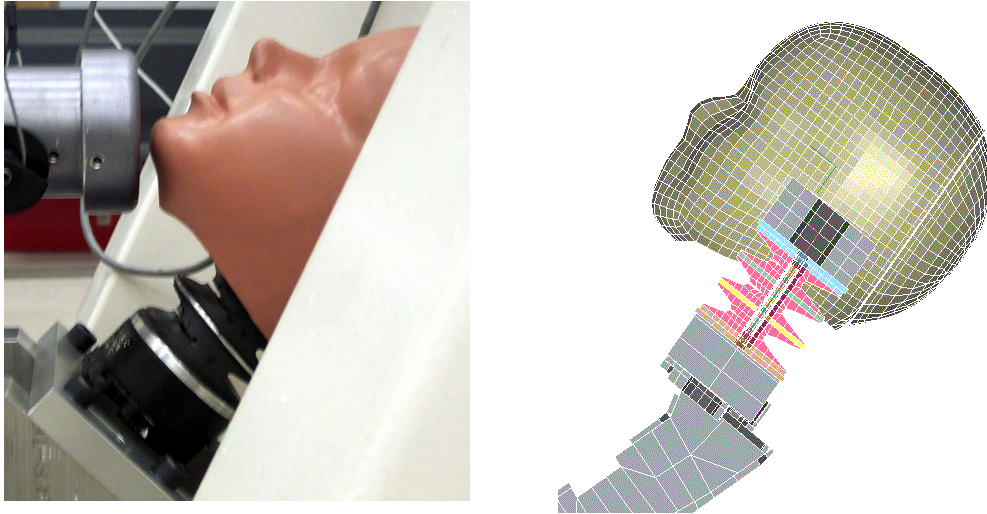


Figure 10: Dummy head and neck in angular position. Hardware (left [10]) and model A (right).

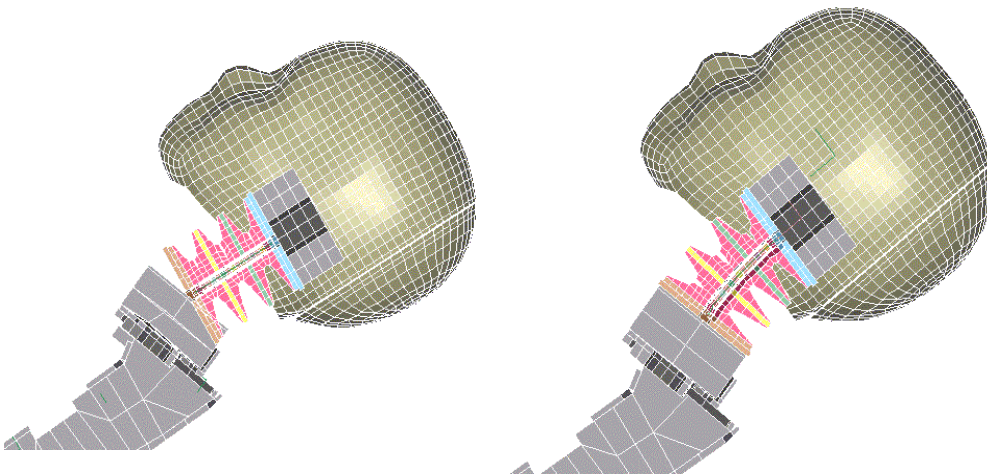


Figure 11: Dummy head and neck in angular position. Neck adapted by a simple preprocessing procedure using a “virtual” joint (left, model B), neck curvature determined by a pre-simulation (right, model C).

SAE 300 filtered	Acceleration [g]		Neck moments [Nm]		Neck forces [kN]	
	Head	Pendulum	Lower	Upper	Lower	Upper
Model A	63	105	-12 / 0	-7.2 / 0	2.1	2.0
Model B	63	106	-13 / 0	-7.3 / 0	2.1	2.0
Model C	58	115	-15 / 0	-2.1 / 4	1.9	1.8
Model D	57	113	-17 / -3	-2.7 / 3	1.9	1.8

Table 7: Results of child neck test. Load level 1.

SAE 300 filtered	Acceleration [g]		Neck moments [Nm]		Neck forces [kN]	
	Head	Pendulum	Lower	Upper	Lower	Upper
Model A	260	200	-32 / 0	0 / 14	9.6	8.7
Model B	227	145	-48 / 13	-30 / 0	8.1	7.8
Model C	227	168	-43 / 0	-28 / 7	8.3	7.6
Model D	226	165	-46 / -3	-27 / 7	8.1	7.5

Table 8: Results of child neck test. Load level 2.

SAE 300 filtered	Acceleration [g]		Neck moments [Nm]		Neck forces [kN]	
	Head	Pendulum	Lower	Upper	Lower	Upper
Model C	58	115	-9.6 / 0	-2.6 / 2	1.6	1.6
Model D	62	114	-11/-3	-3.7 / 1	1.6	1.6

Table 9: Results of child neck test. Load level 1, spine not fixed.

SAE 300 filtered	Acceleration [g]		Neck moments [Nm]		Neck forces [kN]	
	Head	Pendulum	Lower	Upper	Lower	Upper
Model A	204	204	-27 / 0	0 / 13	7.5	7.1
Model B	163	145	-26 / 20	-28 / 0	6.0	6.0
Model C	173	169	-31 / 0	-22 / 6	6.5	6.2
Model D	172	166	-33 / -3	-24 / 5	6.4	6.0

Table 10: Results of child neck test. Load level 2, spine not fixed.

Model A behaves different in all simulations. The cause lies in the significant difference in geometry since the influence of gravity is neglected entirely. The pendulum impact direction is towards the upper neck load cell and small differences of the head rotation may result in an impact above or below the load cell. Since for model A the head has a significant different angle in space, the impact force generates a different kinematics of the head and neck. The models B, C, and D show a much closer behavior, even if the angle of the head is not exactly the same for model B and C. The runs with the high load level and the fixed spine show only minor differences, as outlined in Table 8. The runs with the not fixed spine show approximately 20% difference in the neck moments between model B and C. This shows that the adaptation of the geometry by a “virtual” joint can lead to less predictive models. The similar behavior of model B and C in Table 7 and 8 and the significantly different behavior in Table 10 show also the importance of choosing sensitive tests. Without Table 10 we might have concluded wrongly that the “virtual” joint of model B is sufficient to model the bending of the neck.

Regarding the initial stresses all considered load cases show a limited sensitivity in the lower neck moment. For final assessment investigations with load cases more close to the deployment of an airbag are necessary. In particular the relation between moment and forces in the neck is different in many Out-of-Position load cases.

Conclusions

Different components of dummy models have been analyzed to assess the influence of pre-stress on the injury criteria. The examples considered for the lower spine model of the USSID and the neck of the ES-2 show no major influence in the considered tests. It is likely that they can be neglected. For the child dummy model a limited influence was observed, but due to the simple load cases a final assessment necessitates further investigations.

The load levels in all examples are chosen to be close to real loading scenarios, but in particular for the child model compromises were made. For the child model simulations with the fully assembled models and with loads more close to real airbag loads should be considered for a final assessment. The simulations showed clearly the importance of modeling the exact initial position. For predictive simulations the proper modeling of the bended neck seems indispensable.

The examples for the foam of the HIII pelvis model show more sensitivity regarding the initial stresses. If the foam is compressed in the dynamic load case the stresses can not be neglected. Including only the strains and neglecting the stress in the pelvis foam leads to less accurate results than neglecting both stresses and strains. For low foam compressions no significant influence of the initial conditions was observed. The test considered for the pelvis foam was very simple and further analyzes might be reasonable to estimate the importance of the effect in real loads. In particular for the side impact dummy models further investigations are of interest.

All conclusions are based on dummy models that have been developed with fewer demands on the quasi-static behavior of the material properties. Since the exact initial position is often crucial for the child model a proper static behavior of the models should be implemented in the near future.

With the possibility of implicit time-stepping LS-DYNA provides a perfect tool to determine the initial conditions of the dynamic load case with affordable computational time. LS-DYNA offers also different solutions to include pre-stress and pre-strain in the model. The most general and accurate approach is to include the dummy model and his condition with a full restart. With this approach the pre-simulation has to be performed only once. The results from the pre-simulation can be used seamlessly to analyze and optimize variations of the restraint system effectively.

References

1. DYNAtools, tools available at no cost from Kurt Schweizerhof to be used in connection with LS-DYNA.
2. FAT USSID model for LS-DYNA, Release 4.5.7, developed by DYNAmore GmbH.
3. FAT ES-2 model for LS-DYNA, Release 2.0, developed by DYNAmore GmbH
4. FRANZ U., GRAF O., HIRTH A., REMENSPERGER R., (2001), „Entwicklung von detaillierten LS-DYNA Seitencrashdummies im Rahmen eines FAT-Projektes, Aspekte der Validierung“, Tagung Crashsimulation, Haus der Technik Essen.
5. FRANZ U., SCHMID W., SCHUSTER P. (2002), “Observations During Validation of Side Impact Dummy Models - Consequences for the Development of the FAT ES-2 Model”, Nordic LS-DYNA User Conference, Gothenburg, Sweden.
6. FRANZ U., SCHUSTER P., SCHMID W., GRAF O. (2003), “FAT Side Impact Dummy models – Remarks on usage and potential Pitfalls”, 4th European LS-DYNA User Conference, Ulm, Germany.
7. FTSS HIII 50% model, Release 3.1.
8. FTSS HIII 3 year model, Release 3.0.
9. GRAF O., FRANZ U., SCHMID W., SCHUSTER P. (2003), „Development of the FAT Dummy Models”, LS-DYNA Korean Conference, Seoul, Korea.
10. HUANG Y., HIRTH A., Private communications.
11. LUND A., (2003), “Recommended Procedures for Evaluating Occupant Injury Risk from Deploying Side Airbags”, First Revision.
12. User Manual ES-2 (2002), FTSS Inc.
13. LS-DYNA Keyword Users Manual, Version 970.

